

# Dynamic Changes of the Phosphoproteome in Postmortem Mouse Brains

Tsutomu Oka<sup>1</sup>, Kazuhiko Tagawa<sup>1</sup>, Hikaru Ito, Hitoshi Okazawa\*

Department of Neuropathology, Medical Research Institute, Tokyo Medical and Dental University, Tokyo, Japan

## Abstract

Protein phosphorylation is deeply involved in the pathological mechanism of various neurodegenerative disorders. However, in human pathological samples, phosphorylation can be modified during preservation by postmortem factors such as time and temperature. Postmortem changes may also differ among proteins. Unfortunately, there is no comprehensive database that could support the analysis of protein phosphorylation in human brain samples from the standpoint of postmortem changes. As a first step toward addressing the issue, we performed phosphoproteome analysis with brain tissue dissected from mouse bodies preserved under different conditions. Quantitative whole proteome mass analysis showed surprisingly diverse postmortem changes in phosphoproteins that were dependent on temperature, time and protein species. Twelve hrs postmortem was a critical time point for preservation at room temperature. At 4°C, after the body was cooled down, most phosphoproteins were stable for 72 hrs. At either temperature, increase greater than 2-fold was exceptional during this interval. We found several standard proteins by which we can calculate the postmortem time at room temperature. The information obtained in this study will be indispensable for evaluating experimental data with human as well as mouse brain samples.

**Citation:** Oka T, Tagawa K, Ito H, Okazawa H (2011) Dynamic Changes of the Phosphoproteome in Postmortem Mouse Brains. PLoS ONE 6(6): e21405. doi:10.1371/journal.pone.0021405

**Editor:** Andrea C. LeBlanc, McGill University, Canada

**Received:** March 17, 2011; **Accepted:** May 27, 2011; **Published:** June 22, 2011

**Copyright:** © 2011 Oka et al. This is an open-access article distributed under the terms of the Creative Commons Attribution License, which permits unrestricted use, distribution, and reproduction in any medium, provided the original author and source are credited.

**Funding:** This study was supported by the Strategic Research Program for Brain Sciences (SRPBS) to H.O. from the Ministry of Education, Culture, Sports, Science and Technology (MEXT). The funders had a role in the decision of study direction but no role in study design, data collection and analysis, decision to publish, or preparation of the manuscript.

**Competing Interests:** The authors have declared that no competing interests exist.

\* E-mail: okazawa-ky@umin.ac.jp

These authors contributed equally to this work.

## Introduction

Protein phosphorylation has been implicated widely in the pathological mechanisms of neurodegenerative disorders including Alzheimer's disease (AD), frontotemporal dementia (FTD), dementia with Lewy bodies (DLB), Parkinson's disease dementia (PDD), and Huntington's disease (HD). For instance, hyperphosphorylated forms of tau have been identified as a major component of paired helical filament (PHF) [1], the common pathological hallmark of AD and tau-associated FTD. Hyperphosphorylation impairs the microtubule binding of tau and destabilizes microtubules. A process mediated by various serine/threonine kinases such as GSK3beta, PKA, Cdk5 and casein kinase II might also accelerate aggregation of tau into PHF [2–5]. In the DLB brain, phosphorylated alpha-synuclein at Ser 129 has been detected by mass spectrometry and phosphorylation-accelerated aggregation of alpha-synuclein has been shown *in vitro* [6]. The increase of toxicity by phosphorylation was also suspected in a *Drosophila* model of PDD [7].

However, the significance of variable phosphorylation levels of inclusion body component proteins remains controversial. For instance, in alpha-synuclein, phosphorylated tyrosine and serine residues seem to have opposite effects on cellular toxicity [8]. In addition, the role of phosphorylation can differ among neurodegenerative diseases. In contrast to the cases of tau and synuclein, phosphorylation of mutant huntingtin (Htt) at Ser 421 in response to IGF treatment reduced toxicity [9]; similarly, phosphorylation

of Htt at Ser 13 and 16 alleviated phenotype in a mouse model of HD [10].

Furthermore, one can easily imagine that a number of phosphoproteins other than aggregated proteins would quantitatively change in the context of neurodegenerative disorders. It is possible that such phosphorylation also affects neurodegeneration. Therefore, in order to understand the whole scheme of pathological functions of protein phosphorylation, it is necessary to perform a full “omics” analysis of phosphoproteins in human brains.

However, the most significant obstacle to this approach is posed by the preservation conditions of human brains. There is no world standard that specifies how to preserve postmortem human bodies before the brains are cut, frozen and kept in the brain bank. After patients' deaths, their bodies are left on their beds at room temperature for different length of time before being transferred to the morgue in the pathology department. The time between brain sectioning and freezing on dry ice also varies among samples and among institutions.

Therefore, we need to know how the phosphoproteome changes in postmortem brains during the process of preservation. Based on such knowledge, we could potentially design a specific preservation protocol for brain banks to follow in order to enable reproducible phosphoproteome analysis in human samples. Even with such a standard, specific methods for adjusting phosphoproteomic data based on time and temperature would also be required. For these purposes, we performed proteome-wide analyses of phosphopro-

teins on mouse brains that had been kept at room temperature or 4°C for different lengths of time. The results reveal surprisingly diverse patterns of chronological changes of phosphoproteins. Data such as ours will be crucial in interpreting the phosphoprotein data obtained to date, as well as future data, from human brain samples.

## Results

### Diverse changes of postmortem phosphoproteins

To investigate the effect of postmortem time on phosphoproteins before the brain was isolated and frozen, we kept 12 week-old C57BL/6J mice at 25°C or 4°C for a different length of time (0, 3, 12, 72 hrs) after they were sacrificed by deep euthanasia. After the incubation period, the mice were dissected and their brains immediately frozen in liquid nitrogen. The brain samples were thawed at 4°C in T-PER Tissue Protein Extraction Reagent and immediately used for sample preparation, as described in Methods. The quantitative whole proteome mass analysis was performed with Q-STAR (AB SCIEX) and repeated for three sets of samples. Each set included cerebral cortex samples from a mouse body kept at 25°C or 4°C for different lengths of time (0, 3, 12, 72 hrs).

Relative quantity compared to the initial value at 0 hr was obtained for each phosphoprotein, and the mean value among three sets was calculated for each time point and temperature (Figure 1). Surprisingly, the postmortem changes in phosphoproteins showed extreme diversity (Figure 1). When increase and decrease were defined as more than 1.2 and less than 0.8 fold, respectively, 26% of total phosphoproteins decreased rapidly from 0 to 3 hrs, while 17% of proteins increased during this interval at room temperature (25°C). 75% of total phosphoproteins were reduced after more than 12 hrs at room temperature (25°C), but some exceptional phosphoproteins (5.5%) continued to increase from 12 to 72 hrs. In contrast to the pattern at room temperature, 55% of phosphoproteins were relatively stable after more than 12 hrs at 4°C. However, there were also exceptional cases whose levels increased or decreased rapidly.

### Categorization of temperature-dependent changes of phosphoproteins

We suspected that a mixture of different patterns might cause the extreme diversity of chronological changes. Therefore, we categorized the data by cluster analysis. At each temperature, phosphoproteins were classified into four groups (Figure 2). Group A–C showed typical patterns at each temperature, while group D (“miscellaneous”) contained a wide variety of behaviors. At room temperature, Group A exhibited a transient increase and decline after 12 hrs. Group B exhibited a relatively constant and slow decrease until 72 hrs. Group C exhibited a rapid decrease until 12 hrs and a more gradual decrease after 12 hrs. At 4°C, Group A tended to increase slowly; group B was almost stable until 72 hrs; and group C decreased rapidly until 3 hrs and then stabilized.

The classification revealed that in each temperature group, the initial changes in phosphoprotein levels followed diverse paths until 12 hrs. Later than 12 hrs, all phosphoproteins either stabilized or gradually decreased at room temperature. At the same time, there were exceptional proteins whose changes can hardly be expected. These patterns of change were also supported when proteins were classified by the ratio of changes (Figure 3). Until 12 hrs, the percentage of increased ( $X > 1.2$ ), unchanged ( $0.8 < X < 1.2$ ) or decreased ( $X < 0.8$ ) phosphoproteins was almost the same between 25°C and 4°C. However, the percentage of

decreased proteins ( $X < 0.8$ ) increased markedly at times later than 12 hrs at 25°C.

As shown in Figure 2, the pattern for Group B at 25°C looked similar to that of Group B at 4°C. This was also the case for Group C. This impression was supported by a comparison of phosphoproteins belonging to these groups (Figures S1, S2, S3). The comparison also indicated that expression of a majority of proteins was relatively constant, and that chronological change can be expected at both temperatures.

### Selection of standard phosphoproteins

We next selected standard proteins that can be used for quality control of brain tissue even when information about postmortem processing conditions is not available. We first plotted the mean value of each group (Figures 4, 5). The mean value for total protein level declined at 0.006/hr after 12 hrs at 25°C (Figure 4); in contrast, at 4°C, the mean value was stable until 72 hrs (Figure 5). Corresponding to each group, we selected representative proteins that mimicked the pattern of mean values (Figures 4, 5). The standard proteins that represented the decline of total phosphoproteins at room temperature were Glud1, Pascin1 and Snap25. Glud1 is highly expressed in the brain and is known to function as a mitochondrial enzyme converting glutamate to 2-oxoglutarate [11], thereby affecting the blood ammonia level [12]. Pascin1, a neural isoform of Pascin, is a cytoplasmic phosphoprotein involved in vesicle formation [13] and endocytosis regulation [14]. It also interacts with huntingtin at synapses [15]. Snap25 is a membrane-bound pre-synaptic protein and a component of the SNARE complex [16], which is essential for synaptic vesicle fusion [17] and  $Ca^{2+}$  response [18]. On the other hand, the standard proteins representing the stability of total phosphoproteins at 4°C were Pascin1, Eefeld and Prpsap2. Eefeld delivers aminoacyl tRNAs to the ribosome [19], and is also known to catalyze the exchange of GDP bound to Elongation Factor 1 $\alpha$  with GTP [20] which is stimulated by PKC [21]. Prpsap2 negatively regulates phosphoribosyl pyrophosphate (PRPP) synthetase [22]. These data together indicate that Pascin1 is a good control protein to use in evaluation of the postmortem interval during which the body was left at room temperature before transfer to the morgue in the pathology department.

We also found several phosphoproteins that were relatively stable up to 72 hrs at room temperature (Figure 6). Importantly, one of them, Gm5506 ( $\alpha$ -enolase) was stable also at 4°C (Figure 6). As shown in Figures 4 and 5, the change of Pascin1 exactly matches with the average change of total phosphoprotein (Figures 4, 5). Pascin1 decreases at a constant rate at room temperature but it is stable at 4°C for 72 hrs. In contrast, Gm5506 is stable both at room temperature and 4°C. The ratio between the absolute signal values of Pascin1 and Gm5506 at 0 hr (76.1:75.1) is also known. From these values, we can calculate the postmortem time at room temperature according to the formula (Figure 7).

## Discussion

This study had three main goals: 1) to investigate how the phosphoproteome is changed in postmortem brains over the course of preservation; 2) to propose a specific preservation protocol that is suitable for phosphoproteome analysis of brain tissue; 3) to develop a specific method for adjusting phosphoprotein data based on time and temperature. For these purposes, we performed whole-proteome analyses of phosphoproteins using mouse brains that had been kept at room temperature or 4°C for different lengths of time.

	Fidelity	Protein	Peptide
Set 1	>99%	63	5221
	>95%	92	7119
	>66%	110	8430
	>10%	136	10233
Set 2	>99%	43	4540
	>95%	65	5967
	>66%	90	7579
	>10%	118	9537
Set 3	>99%	36	3375
	>95%	58	4756
	>66%	70	5438
	>10%	88	6664

	Fidelity	Protein	Peptide
total	>99%	85	10397
	>95%	126	14054
	>66%	158	16779
	>10%	190	20436

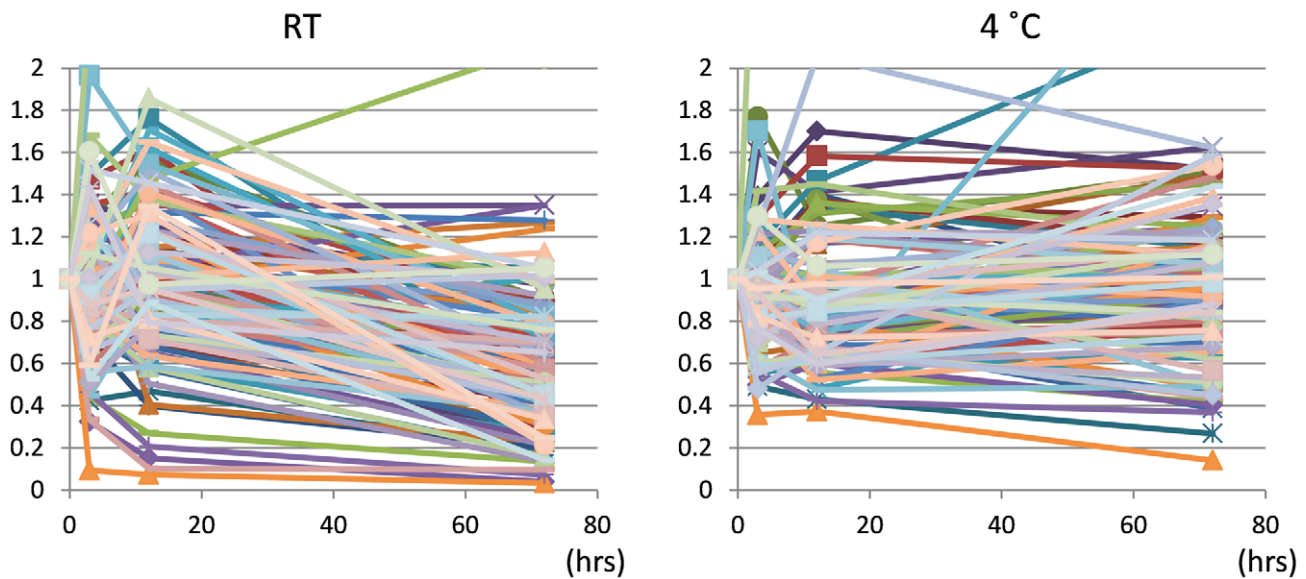


**Figure 1. Postmortem dynamics of phosphoproteins revealed by quantitative mass analysis.** The numbers of proteins and peptides identified from three sets of mass analysis are listed. 126 proteins were identified with more than 95% fidelity from the merged data of three sets. The lower graphs show the chronological change of phosphoproteins during preservation at 25°C and 4°C. doi:10.1371/journal.pone.0021405.g001

First, we learned that the chronological changes in phosphoproteins are surprisingly diverse. Most proteins (82.5% at RT and 93.7% at 4°C) change following several typical patterns (Group A, B or C). However, the change of the other proteins is hardly prospected (Group D). This result suggests several things. If a phosphoprotein of interest belongs to the three regular groups (Groups A–C), we can evaluate whether the value obtained in an experiment is increased or decreased based on the pattern obtained in this study. If a target phosphoprotein in future research belongs to Group D, however, caution must be taken in evaluating its levels. Although the patterns are limited to 126 proteins in our current study, the database would be expanded to a larger number of phosphoproteins. We are now obtaining data with a higher grade of mass analysis; the results will be made available as an open database in the future.

As hyperphosphorylation of some specific proteins has been implicated as causative in neurodegenerative disorders, we asked whether our current results included such important proteins. However, APP [23-27], Presenilin1/2 [28,29], tau [30,31], Apolipoprotein E [32], Cdk5 [33], TDP-43 [34] or GSK-3beta [35], which are implicated in Alzheimer’s disease and tauopathy, were not included in these results. Also, alpha-synuclein [36,37], Leucine-rich repeat kinase 2 [38,39], ubiquitin carboxyl-terminal hydrolase L1 [40], Parkin [41], Pink1 [42], Grb10-Interacting GYF Protein-2 [43], or Omi/HtrA2 [44], which are implicated in Parkinson’s disease, are not included. The postmortem changes in these proteins will also become clear in a future study.

Although postmortem changes in phosphoproteins were diverse over the first 12 hrs, they were generally inclined to decrease from 12 to 72 hrs. Since only one protein was increased more than

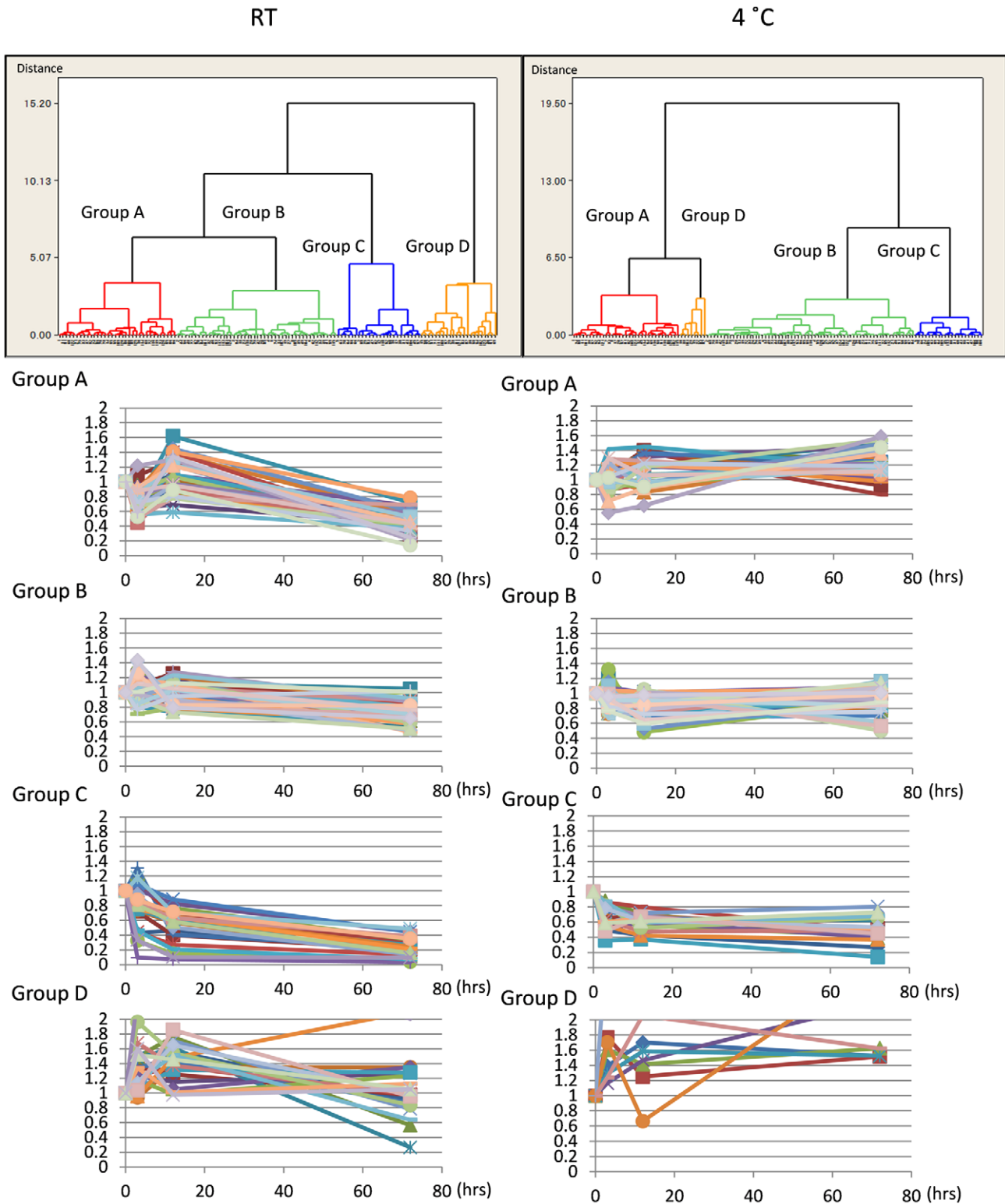


**Figure 2. Cluster analysis of postmortem phosphoprotein dynamics.** Dendrograms of total identified proteins at RT (25°C) and 4°C were drawn by cluster analysis. Cerebral cortex phosphoproteins were classified into four groups according to the changing pattern (upper panels). At 25°C, 34, 46, 24 and 22 proteins belong to Groups A, B, C and D, respectively. At 4°C, 33, 64, 21 and 8 proteins belong to Groups A, B, C and D, respectively. Lower graphs show the patterns of chronological change for phosphoproteins in each group. doi:10.1371/journal.pone.0021405.g002

Distribution of the quantitative ratio

	3hrs RT	3hrs 4 °C	12hrs RT	12hrs 4 °C	72hrs RT	72hrs 4 °C
1.2<X	16.67%	11.11%	25.40%	16.67%	5.56%	19.84%
0.8<X<1.2	57.14%	63.49%	49.20%	46.83%	19.84%	54.76%
X<0.8	26.19%	25.40%	25.40%	36.50%	74.60%	25.40%
mean	0.9611	0.9431	1.0085	0.9256	0.6241	0.9795
(SD)	(0.3078)	(0.3018)	(0.3726)	(0.3174)	(0.3474)	(0.3741)

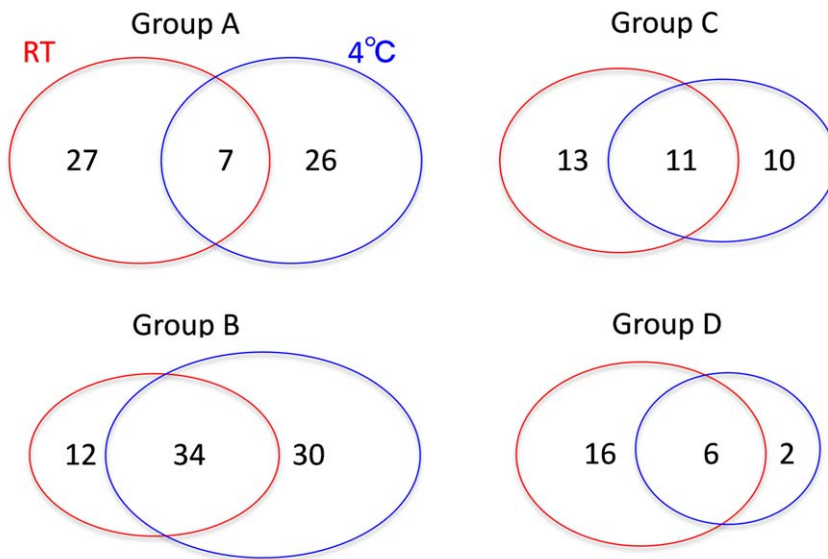


**Figure 3. Comparison between RT and 4°C groups.** (A) Identified phosphoproteins at each time point were classified into three groups based on the relative quantity to the initial value at 0 hr. (B) Corresponding groups are compared between RT (25°C) and 4°C to evaluate the similarity between groups.  
doi:10.1371/journal.pone.0021405.g003

2-fold during 72 hrs at room temperature, and only two proteins were increased more than 2-fold during 72 hrs at 4°C, increases more than 2-fold can be suspected as abnormal in any postmortem samples that were kept at 4°C within 72 hrs. However, after getting such a result, one should come back to postmortem omics data such as ours in order to check the validity of the result.

Second, we can now propose how the brain samples should be prepared for the analysis of phosphoproteins. Our results showed that some proteins rapidly decreased within 12 hrs at room temperature (Figure 2, Group C at RT) while some other proteins increased within 12 hrs at room temperature (Figure 2, Group A at RT). After 12 hrs, most phosphoproteins declined at a constant rate (0.006/ hr), and we learned that the mean value of phosphoproteins at room temperature was remarkably decreased at 72 hrs (Figure 3).

Even at 4°C, some proteins were increased or decreased within 12 hrs (Figure 2, Groups A–C at 4°C). Later than 12 hrs, however, the amounts of phosphoprotein were very stable (Figure 2, Groups A–C at 4°C). This probably means that it takes some time before the brain temperature reaches 4°C, and some phosphoproteins change quantitatively during the time. But after the brain temperature was brought to 4°C, phosphoproteins were stable until 72 hrs. Measurement of postmortem deep brain temperature supported this speculation (Figure S4).

Thus, the body should be chilled to 4°C as soon as possible, no later than 12 hrs after death. In other words, the brain temperature should become 4°C within 12 hrs postmortem. Even with more or less immediate chilling, however, one should refer to our database in this study (Figure S5) showing how each phosphoprotein changes over the course of the first 12 hrs. We will update the database, covering far more phosphoproteins, in the near future.

Third, we propose a method for estimating the postmortem time spent at room temperature. Pascin1 decreases at a constant rate at room temperature, exactly matching with the average change of total phosphoprotein (Figures 4, 5). In addition, Pascin1 is stable at 4°C for 72 hrs. In contrast, Gm5506 is stable both at room temperature and 4°C. The absolute signal value ratio between Pascin1 and Gm5506 at 0 hr (76.1:75.1) is also known. Therefore, we could calculate the postmortem time at room temperature from these values (Figure 7). We would be able to use Eefeld and Prpsap2, as well as Hspa8/Hsp70-4 or 14-3-3  $\alpha/\beta$ , as other standards for the same purpose. If we can obtain a fresh human brain sample and measure the absolute ratio between Pascin1 and Gm5506/ $\alpha$ -enolase at 0 hr, this method can be used to calculate the postmortem time in humans. However, for ethical reasons, we have not obtained such a value currently.

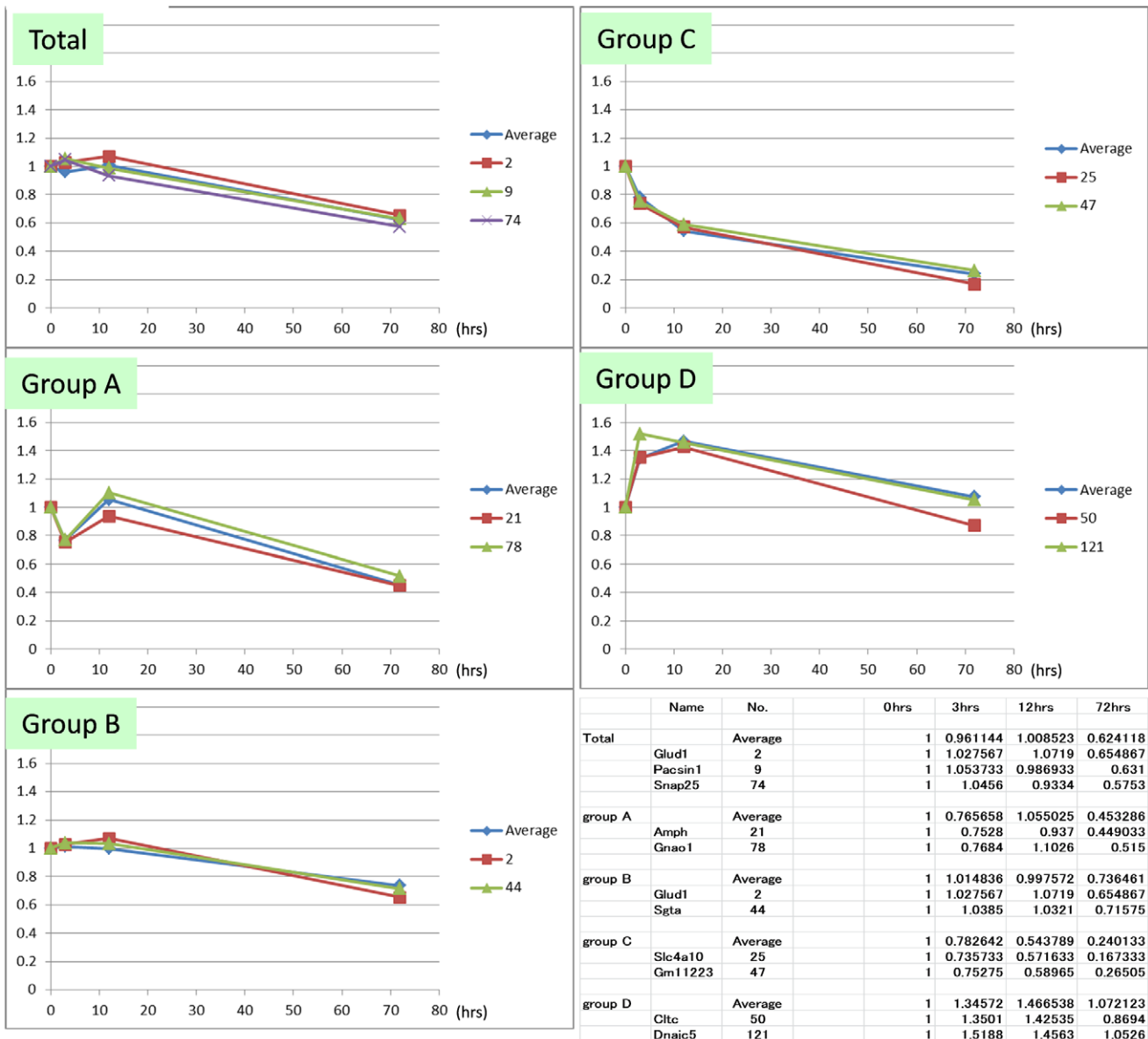


**Figure 4. Representative genes of each clustered group at RT.** Chronological changes at 25°C of the mean value of total identified phosphoproteins (Total) and of phosphoproteins belonging to each group (Groups A–D) are shown. Proteins most similar to the mean value pattern were also selected.

doi:10.1371/journal.pone.0021405.g004

This study left several issues for future studies. First, we may have to add earlier time points to detect certain unexpected changes of phosphoproteins. Second, we need to analyze other parts of the brain like brainstem, cerebellum, and spinal cord. The dynamics of phosphoproteins in such brain parts might be different from that of cerebral cortex. The information will be necessary for the phosphoprotein in human diseases like spinocerebellar ataxia or multiple system atrophy.

In conclusion, our data has provided crucial information that can be used to interpret future data, as well as previously reported experimental data regarding phosphoproteins. We may have to re-evaluate previous reports using human samples from the standpoint of postmortem time and temperature. Future experiments using human samples should definitely be evaluated using our data, which will be expanded and delivered as an open database.

## Materials and Methods

### Ethics statement

All procedures were approved by the Institutional Animal Care and Use Committee of the Tokyo Medical and Dental University (MR:2010-002) and performed according to the guidelines of Ministry of Education, Culture, Sports, Science and Technology (MEXT) of Japanese government.

### Sample preparation

12 week-old C57BL/6J mice were kept at 25°C or 4°C for different lengths of time (0, 3, 12, 72 hrs) after they were sacrificed by deep euthanasia using ethyl ether. Mice were put in a glass bottle (5L) in which the air was saturated by ethyl ether. The mice were deeply anesthetized by ether vapor at three minutes later

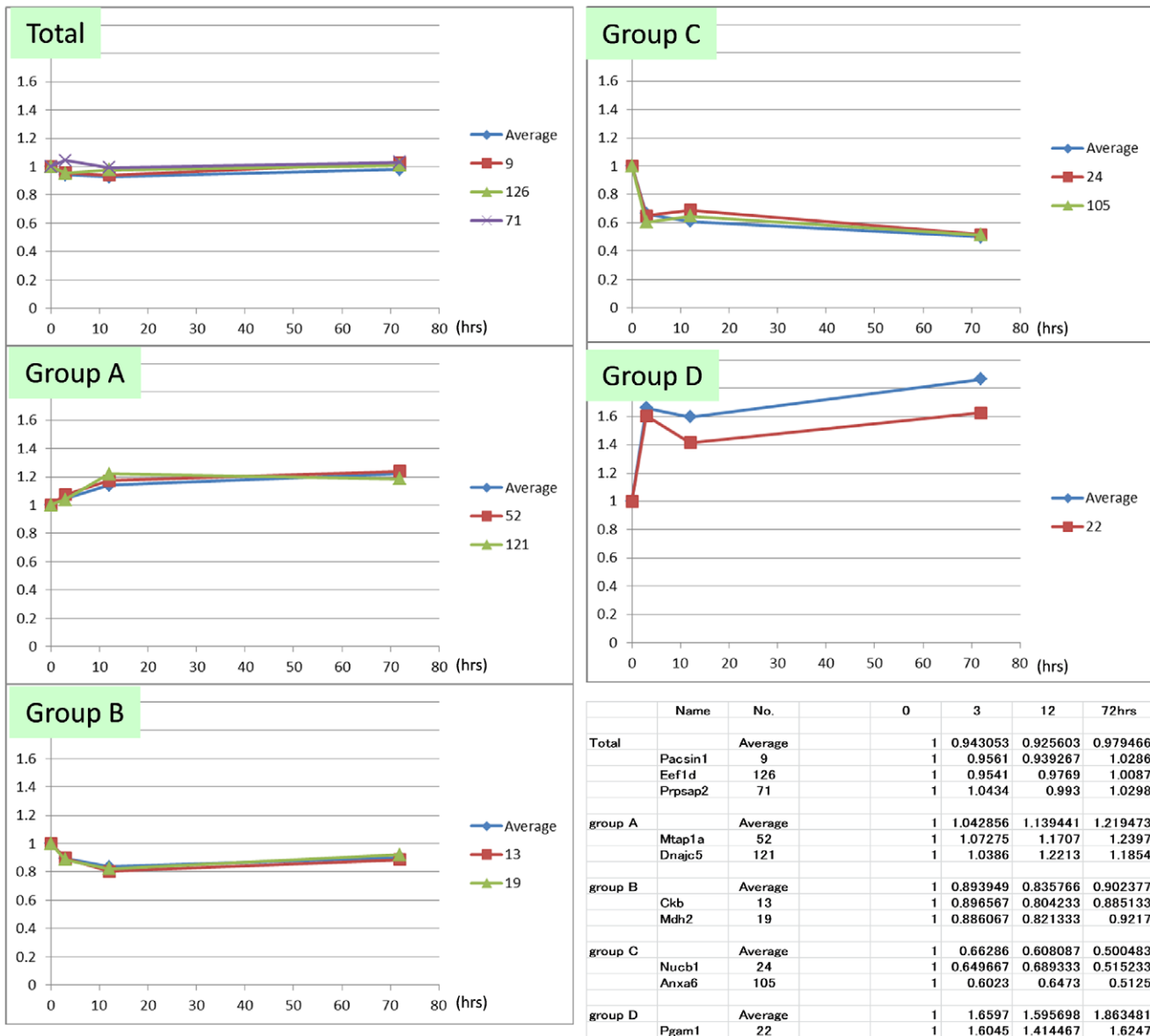


**Figure 5. Representative genes of each clustered group at 4°C.** Chronological changes at 4°C of the mean value of total identified phosphoproteins (Total) and of phosphoproteins belonging to each group (Groups A–D) are shown. Representative proteins that mimic the mean value pattern are also selected. doi:10.1371/journal.pone.0021405.g005

when they were sacrificed. Their cerebral cortex was isolated, immediately frozen in liquid nitrogen, and stored at -80°C. Protein was extracted from the cerebral cortex using the T-PER Tissue Protein Extraction Reagent (Thermo Fisher Scientific Inc., USA). The amount of the protein was measured using the BCA Protein Assay Reagent (Thermo Fisher Scientific Inc.).

**iTRAQ labeling**

Samples containing 95 µg of protein were denatured in 0.1% SDS, and reduced in 5 mM TCEP (tris-2-carboxyethyl phosphine) for 1 hr at 60°C. Cysteine residues were blocked with 10 mM MMTS (methyl methanethiosulfonate) for 10 min at 25°C, and then samples were digested with trypsin (10:1 protein/enzyme w/w) for 24 hrs at 37°C. The digested proteins (peptides) were then passed through a Sep-Pak Light C18 cartridge column (Waters Corporation, USA) to be desalted. Phosphopeptides were enriched

using the Titansphere Phos-Tio Kit (GL Sciences Inc., Japan), and desalted again with a Sep-Pak Light C18 cartridge column. The peptides in each individual sample were labeled separately using the iTRAQ Reagent-multiplex assay kit (AB SCIEX Ins.) for 2 hrs at 25°C. The labeled peptide pools were then mixed together. Next, the peptide mixture was subjected to SCX (Strong Cation Exchange) chromatography (AB SCIEX Ins.). The peptide mixture was eluted in a stepwise gradient from 20, 60, 100, 150, 200, and 350 mM KCl in 10 mM KH<sub>2</sub>PO<sub>4</sub> (pH 3.0), 25% acetonitrile. The peptide fractions were dried and desalted using a Sep-Pak Light C18 cartridge column.

**Quantitative whole proteome mass analysis**

The dried peptide fractions were re-suspended in 2% acetonitrile and 0.1% formic acid. Each SCX fraction was analyzed using a DiNa Nano-flow LC system (KYA Technologies

RT

No.	Name	0	3	12	72 hrs
18	Hspa8	1	1.1374	1.138967	0.9063
23	Gm5506	1	1.113767	1.128133	1.049633
28	Aldoa	1	1.061	1.0814	0.865233
42	Eno2	1	1.0397	1.06245	0.84705
67	Rab10	1	0.8911	1.0948	0.8077
79	14-3-3 beta/alpha	1	1.0491	1.0638	0.8889
118	Hba-a2;Hba-a1	1	1.0061	1.1276	1.0067

4 °C

No.	Name	0	3	12	72 hrs
2	Glud1	1	0.811533	0.9143	0.951467
3	Dpysl2	1	0.880233	0.813533	1.001667
9	Pacsin1	1	0.9561	0.939267	1.0286
11	Stx1a	1	1.120733	1.1911	1.0925
13	Ckb	1	0.896567	0.804233	0.885133
16	Prkcb	1	0.949733	1.0232	1.020567
18	Hspa8	1	0.871	0.8657	0.9543
19	Mdh2	1	0.886067	0.821333	0.9217
23	Gm5506	1	1.0343	1.024233	0.956233
25	Slc4a10	1	0.933467	1.021933	0.801533
28	Aldoa	1	0.904133	0.8505	0.995233
36	Sod1	1	1.10045	1.07425	1.1506
40	Ccny	1	0.89465	0.99315	1.01445
42	Eno2	1	0.8318	0.86785	0.9337
46	Atp5b	1	0.83975	1.01365	0.8519
48	Ppia	1	1.0348	0.82955	0.85805
50	Cltc	1	1.1577	0.83205	1.03965
56	Actg1	1	0.80355	0.8643	0.9075
61	14-3-3 epsilon	1	1.0783	1.0142	1.0869
65	Basp1	1	0.8888	0.8284	1.0834
68	Atp5a1	1	0.8105	0.9332	0.9382
71	Prpsap2	1	1.0434	0.993	1.0298
74	Snap25	1	1.0223	1.1903	1.0233
75	Hsp90ab1	1	1.0426	1.0218	1.0554
78	Gnao1	1	0.8238	0.921	1.0046
79	14-3-3 beta/alpha	1	0.8098	0.8843	0.9007
85	Spnb2	1	0.9606	0.8064	1.0885
93	Ap3b2	1	0.9022	0.94	0.8148
96	Gls	1	0.8536	1.0126	0.9177
101	Nlgn2	1	1.1066	1.1939	1.0713
107	Ndr4	1	0.8617	0.9722	0.8219
111	Syn1	1	0.9599	0.8633	1.1397
116	Gpm6b	1	0.9695	0.9712	1.1427
117	Tpm1	1	0.9139	0.9066	0.8419
119	Gm13464	1	0.8151	0.8479	0.9842
126	Eef1d	1	0.9541	0.9769	1.0087

**Figure 6. Stable proteins at RT and 4°C.** Proteins whose relative amount stayed within 0.8 to 1.2 during 72 hrs are listed. 7 and 36 proteins matched this criterion at 25°C and 4°C, respectively. Proteins found at both temperatures are marked in red. Arrows indicate the standard protein, which is stable at RT (25°C) and 4°C.  
doi:10.1371/journal.pone.0021405.g006


Corporation, Japan) and Q-STAR® Elite Hybrid LC/MS/MS System (AB SCIEX Ins.). The samples were loaded onto a 0.1 mm×100 mm C18 column and eluted with a gradient of

5–100% solution B (80% acetonitrile and 0.1% formic acid) in solution A (2% acetonitrile and 0.1% formic acid). The flow rate was 300 nL/min, and ion spray voltage was 1.8 kV. The IDA



Time at RT (hour) =

$$\frac{1}{0.006} \times \left[ 1 - \frac{75.1}{76.1} \times \frac{\text{Pacsin1}}{\text{Gm5506}} \right] + 12$$


  
 $\frac{\text{Pacsin1 (0 hour)}}{\text{Gm5506 (0 hour)}}$

**Figure 7. The formula for calculating the postmortem time at room temperature.** The formula was based on the characters of Pacsin1 and Gm5506. Pacsin1 decreases at a constant rate at room temperature but it is stable at 4°C for 72 hrs. In contrast, Gm5506 is stable both at room temperature and 4°C. The ratio between Pacsin1 and Gm5506 at 0 hr (76.1:75.1) is also known. If the ratio between Pacsin1 and Gm5506 at 0 hr in fresh human brain samples is known, we can calculate the postmortem time at RT in human brain with the formula.

doi:10.1371/journal.pone.0021405.g007

(Information Dependent Acquisition) setting was 400–1800 *m/z* with two to four charges. Analyst QS 2.0 software (AB SCIEX Ins.) was used to identify each peptide. Quantification of each peptide was based on TOF-MS electric current detected during the LC-separated peptide peak, adjusted by the charge/peptide ratio. Quantification of a protein was deduced by averaging the quantities of multiple peptide peaks from the protein. These processes were automatically performed using the Q-STAR® Elite Hybrid LC/MS/MS Hybrid System (AB SCIEX Ins.)

## References

- Nukina N, Ihara Y (1985) Proteolytic fragments of Alzheimer's paired helical filaments. *J Biochem* 98: 1715–1718.
- Masliah E, Iimoto DS, Mallory M, Albright T, Hansen L, et al. (1992) Casein kinase II alteration precedes tau accumulation in tangle formation. *Am J Pathol* 140: 263–268.
- Hanger DP, Byers HL, Wray S, Leung KY, Saxton MJ, et al. (2007) Novel phosphorylation sites in tau from Alzheimer brain support a role for casein kinase I in disease pathogenesis. *J Biol Chem* 282: 23645–23654.
- Wang JZ, Grundke-Iqbal I, Iqbal K (2007) Kinases and phosphatases and tau sites involved in Alzheimer neurofibrillary degeneration. *Eur J Neurosci* 25: 59–68.
- Piedrahita D, Hernández I, López-Tobón A, Fedorov D, Obara B, et al. (2010) Silencing of CDK5 reduces neurofibrillary tangles in transgenic Alzheimer's mice. *J Neurosci* 30: 13966–13976.
- Fujiwara H, Hasegawa M, Dohmae N, Kawashima A, Masliah E, et al. (2002) alpha-Synuclein is phosphorylated in synucleinopathy lesions. *Nat Cell Biol* 4: 160–164.
- Chen L, Feany MB (2005) Alpha-synuclein phosphorylation controls neurotoxicity and inclusion formation in a *Drosophila* model of Parkinson disease. *Nat Neurosci* 8: 657–663.
- Chen L, Periquet M, Wang X, Negro A, McLean PJ, et al. (2009) Tyrosine and serine phosphorylation of alpha-synuclein have opposing effects on neurotoxicity and soluble oligomer formation. *J Clin Invest* 119: 3257–3265.
- Humbert S, Bryson EA, Cordelières FP, Connors NC, Datta SR, et al. (2002) The IGF-1/Akt pathway is neuroprotective in Huntington's disease and involves Huntingtin phosphorylation by Akt. *Dev Cell* 2: 831–837.
- Gu X, Greiner ER, Mishra R, Kodali R, Osmand A, et al. (2009) Serines 13 and 16 are critical determinants of full-length human mutant huntingtin induced disease pathogenesis in HD mice. *Neuron* 64: 828–840.
- Palaiologos G, Hertz L, Schousboe A (1988) Evidence that aspartate aminotransferase activity and ketodicarboxylate carrier function are essential for biosynthesis of transmitter glutamate. *J Neurochem* 51: 317–320.

## Cluster analysis of identified proteins

The quantitative ratio between 0 hr and the other 6 time points (1, 25°C for 3 hrs; 2, 25°C for 12 hrs; 3, 25°C for 72 hrs; 4, 4°C for 3 hrs; 5, 4°C for 12 hrs; 6, 4°C for 72 hrs) in each detected protein was obtained using the Protein Pilot software (AB SCIEX Ins.) analysis. The chronological pattern was classified into four groups by clustering analysis using Minitab 16 software with the Ward method and Euclidean distance. Dendrograms were drawn using the same software.

## Supporting Information

**Figure S1** Proteins belonging to each cluster group at 25°C are listed. Proteins that are members of the same groups at 25°C and 4°C are marked in red.

(TIF)

**Figure S2** Proteins belonging to each cluster group at 4°C are listed. Proteins that are members of the same groups at 25°C and 4°C are marked in red.

(TIF)

**Figure S3** Full names of the gene symbols, listed in alphabetical order.

(TIF)

**Figure S4** Chronological change of the deep brain temperature in mouse body at 25°C or 4°C. Temperature was measured using a needle thermometer (Testo 905-T1, Japan) in mouse bodies left at 25°C or 4°C and mean +/- SD (n = 4) are shown in the graph.

(TIF)

**Figure S5** The Excel file includes all the data on 126 proteins.

(TIF)

## Author Contributions

Conceived and designed the experiments: HO. Performed the experiments: TO KT HI. Analyzed the data: TO KT. Wrote the paper: TO HO.

22. Katashima R, Iwahana H, Fujimura M, Yamaoka T, Ishizuka T, et al. (1998) Molecular cloning of a human cDNA for the 41-kDa phosphoribosylpyrophosphate synthetase-associated protein. *Biochim Biophys Acta* 1396: 245–250.
23. Kang J, Lemaire HG, Unterbeck A, Salbaum JM, Masters CL, et al. (1987) The precursor of Alzheimer's disease amyloid A4 protein resembles a cell-surface receptor. *Nature* 325: 733–736.
24. Tarr PE, Contursi C, Roncarati R, Noviello C, Ghersi E, et al. (2002) Evidence for a role of the nerve growth factor receptor TrkA in tyrosine phosphorylation and processing of beta-APP. *Biochem Biophys Res Commun* 295: 324–329.
25. Tarr PE, Roncarati R, Pelicci G, Pelicci PG, D'Adamio L (2002) Tyrosine phosphorylation of the beta-amyloid precursor protein cytoplasmic tail promotes interaction with Shc. *J Biol Chem* 277: 16798–16804.
26. Russo C, Dolcini V, Salis S, Venezia V, Zambrano N, et al. (2002) Signal transduction through tyrosine-phosphorylated C-terminal fragments of amyloid precursor protein via an enhanced interaction with Shc/Grb2 adaptor proteins in reactive astrocytes of Alzheimer's disease brain. *J Biol Chem* 277: 35282–35288.
27. Takahashi K, Niidome T, Akaike A, Kihara T, Sugimoto H (2008) Phosphorylation of amyloid precursor protein (APP) at Tyr687 regulates APP processing by alpha- and gamma-secretase. *Biochem Biophys Res Commun* 377: 544–549.
28. Kang DE, Soriano S, Xia X, Eberhart CG, De Strooper B, et al. (2002) Presenilin couples the paired phosphorylation of beta-catenin independent of axin: implications for beta-catenin activation in tumorigenesis. *Cell* 110: 751–762.
29. Kuo LH, Hu MK, Hsu WM, Tung YT, Wang BJ, et al. (2008) Tumor necrosis factor-alpha-elicited stimulation of gamma-secretase is mediated by c-Jun N-terminal kinase-dependent phosphorylation of presenilin and nicastrin. *Mol Biol Cell* 19: 4201–4212.
30. Iqbal K, Grundke-Iqbal I, Smith AJ, George L, Tung YC, et al. (1989) Identification and localization of a tau peptide to paired helical filaments of Alzheimer disease. *Proc Natl Acad Sci U S A* 86: 5646–5650.
31. Grundke-Iqbal I, Iqbal K, Tung YC, Quinlan M, Wisniewski HM, et al. (1986) Abnormal phosphorylation of the microtubule-associated protein tau (tau) in Alzheimer cytoskeletal pathology. *Proc Natl Acad Sci U S A* 83: 4913–4917.
32. Strittmatter WJ, Saunders AM, Schmechel D, Pericak-Vance M, Enghild J, et al. (1993) Apolipoprotein E: high-avidity binding to beta-amyloid and increased frequency of type 4 allele in late-onset familial Alzheimer disease. *Proc Natl Acad Sci U S A* 90: 1977–1981.
33. Chang KH, de Pablo Y, Lee HP, Lee HG, Smith MA, et al. (2010) Cdk5 is a major regulator of p38 cascade: relevance to neurotoxicity in Alzheimer's disease. *J Neurochem* 113: 1221–1229.
34. Arai T, Mackenzie IR, Hasegawa M, Nonaka T, Niizato K, et al. (2009) Phosphorylated TDP-43 in Alzheimer's disease and dementia with Lewy bodies. *Acta Neuropathol* 117: 125–136.
35. Noble W, Planel E, Zehr C, Olm V, Meyerson J, et al. (2005) Inhibition of glycogen synthase kinase-3 by lithium correlates with reduced tauopathy and degeneration in vivo. *Proc Natl Acad Sci U S A* 102: 6990–6995.
36. Okochi M, Walter J, Koyama A, Nakajo S, Baba M, et al. (2000) Constitutive phosphorylation of the Parkinson's disease associated alpha-synuclein. *J Biol Chem* 275: 390–397.
37. Polymeropoulos MH, Lavedan C, Leroy E, Ide SE, Dehejia A, et al. (1997) Mutation in the alpha-synuclein gene identified in families with Parkinson's disease. *Science* 276: 2045–2047.
38. Greggio E, Taymans JM, Zhen EY, Ryder J, Vancraenenbroeck R, et al. (2009) The Parkinson's disease kinase LRRK2 autophosphorylates its GTPase domain at multiple sites. *Biochem Biophys Res Commun* 389: 449–454.
39. Mortiboys H, Johansen KK, Aasly JO, Bandmann O (2010) Mitochondrial impairment in patients with Parkinson disease with the G2019S mutation in LRRK2. *Neurology* 75: 2017–2020.
40. Andersson FI, Werrell EF, McMorran L, Crone WJ, Das C, et al. (2011) The Effect of Parkinson's-Disease-Associated Mutations on the Deubiquitinating Enzyme UCH-L1. *J Mol Biol* 407: 261–72.
41. Imam SZ, Zhou Q, Yamamoto A, Valente AJ, Ali SF, et al. (2011) Novel regulation of Parkin function through c-Abl-mediated tyrosine phosphorylation: implications for Parkinson's disease. *J Neurosci* 31: 157–163.
42. Kim Y, Park J, Kim S, Song S, Kwon SK, et al. (2008) PINK1 controls mitochondrial localization of Parkin through direct phosphorylation. *Biochem Biophys Res Commun* 377: 975–980.
43. Lautier C, Goldwurm S, Dürr A, Giovannone B, Tsiras WG, et al. (2008) Mutations in the GIGYF2 (TNRC15) gene at the PARK11 locus in familial Parkinson disease. *Am J Hum Genet* 82: 822–833.
44. Strauss KM, Martins LM, Plun-Favreau H, Marx FP, Kautzmann S, et al. (2005) Loss of function mutations in the gene encoding Omi/HtrA2 in Parkinson's disease. *Hum Mol Genet* 14: 2099–2111.